Rapid Communications

Self-trapping and ordering of heavy holes in the wide band-gap semiconductor β-Ga_2O_3

Igor Altfeder,[1,2,*] Elisabeth Bianco,[1] and Donald L. Dorsey[1]
[1]*Nanoelectronic Materials Branch, Air Force Research Laboratory, Wright-Patterson Air Force Base, Ohio 45433, USA*
[2]*Department of Physics, The Ohio State University, Columbus, Ohio 43210, USA*

(Received 1 June 2018; revised manuscript received 18 September 2018; published 28 December 2018)

Scanning tunneling microscopy (STM) has been utilized for imaging and manipulation of self-trapped holes on the surface of the wide band-gap semiconductor β-Ga_2O_3. A positively charged surface layer comprised of localized holes with 10^{13} cm^{-2} density has been observed for n-doped samples. We show that the surface layer can be populated by hole pumping from the STM tip. A transition between the glassy phase and ordered striped phase of self-trapped holes has also been observed. Our analysis indicates that the saturated two-dimensional density of self-trapped holes may be determined by balance of self-trapping and Coulomb repulsion energies.

DOI: 10.1103/PhysRevB.98.241413

Spontaneous ordering of charge carriers represents one of the most fascinating phenomena in physics. At extremely low densities, charge ordering, also known as Wigner crystallization [1], occurs due to the competition of kinetic $\hbar^2/mR^2$ and Coulomb e^2/R energies, with R being the distance between electrons. In the opposite limit of high carrier densities ($R \sim$ interatomic distance a) and fractional filling, the electronic charge density wave (CDW) develops due to competition of on-site and next-neighbor Coulomb energies of the extended Hubbard model [2]. The experimental observations of these two charge ordering regimes have been reported for two-dimensional (2D) electrons on the surface of liquid helium ($R \sim 100$ nm) [3–9] and in the 2D Mott-Hubbard systems ($R = 2a$) [10]. The intermediate Wigner-Mott regime of charge ordering, with $R \sim$ few nm, would be anticipated for self-trapped charges in wide band-gap semiconductors. For example, in wide band-gap semiconductor β-Ga_2O_3 [11–20], self-trapping of heavy holes due to the formation of Mott polarons [11] has been predicted. Although in the present theory [11] self-trapped holes in β-Ga_2O_3 are considered as individual defects that are not interacting with each other, in principle, significant surface densities of self-trapped holes with significant repulsive Coulomb interactions can be produced by charge pumping from the tip of a scanning tunneling microscope (STM). In other semiconductors, significant ordering tendencies for ensembles of interacting charged polarons were predicted at high densities [21]. The STM technique can be used for experimental verification of hole self-trapping and interaction-induced spatial ordering in wide band-gap semiconductors, including β-Ga_2O_3. It is anticipated that self-trapped charges can manifest on STM images as strong localized signal corrugations, whose lateral dimensions will be determined by spatial extents of the Coulomb fields created by them.

In this Rapid Communication, we report the experimental observation of self-trapped holes using STM on a β-Ga_2O_3 ($\bar{2}01$) surface. Our results indicate that depending on the initial experimental conditions, self-trapped holes can form either a disordered glassy phase or an anisotropically ordered 1D striped phase. The hole self-trapping energy U_0 that is estimated from our STM data is in good agreement with a previous modeling study [11].

The samples for our study were n-type (weakly Sn-doped) β-Ga_2O_3 ($\bar{2}01$) wafers grown by Tamura Corp. (Japan). On as-received samples, the ambient atomic force microscopy (AFM) measurements have shown atomically flat surface geometry. In Fig. 1(a), the AFM image size is $0.5 \times 0.5\,\mu m^2$. As one can conclude from the analysis of AFM cross sections [see Fig. 1(b)], the surfaces of the studied wafers consist of atomically flat terraces and 5 Å height atomic steps. The atomic flatness of ($\bar{2}01$)-oriented samples most likely has to do with the inherent anisotropy of the monoclinic β-Ga_2O_3 lattice. The ($\bar{2}01$) crystal plane for this material represents the plane of easy cleavage. After AFM characterization, the sample was loaded into an ultrahigh vacuum (UHV) chamber, with base pressure 7×10^{-11} Torr, equipped with a scanning tunneling microscope and variable-temperature stage. The samples were annealed in UHV to 350 °C for 24 hours to eliminate the adsorbed water from the surface. The STM measurements were performed at room temperature and the results were reproduced on different samples.

Typical large-view STM images of the postannealed β-Ga_2O_3 ($\bar{2}01$) surface are shown in Figs. 2(a) and 2(b). In Fig 2(a), the image size is $560 \times 560\,nm^2$. The image was obtained using 20 pA current and −5 V sample bias. In Fig. 2(b), the image size is $170 \times 170\,nm^2$, and this image was obtained under the same tunneling current and bias conditions. On STM cross section of this image [see Fig. 2(c)], we observe 3 Å height modulation with typical spatial periodicity of 3 nm developing on top of atomic terraces. The higher-magnification STM image is shown in Fig. 3. In Fig 3, the image size is $74 \times 74\,nm^2$. The image was obtained at 20 pA tunneling current and −4 V sample bias. Please note that the signal modulation observed so far does not reveal any visible spatial order. As we shall later show, the observed 3 nm spaced signal corrugations on top of atomic terraces arise from

*Corresponding author: altfeder.2@osu.edu

 ©2018 American Physical Society

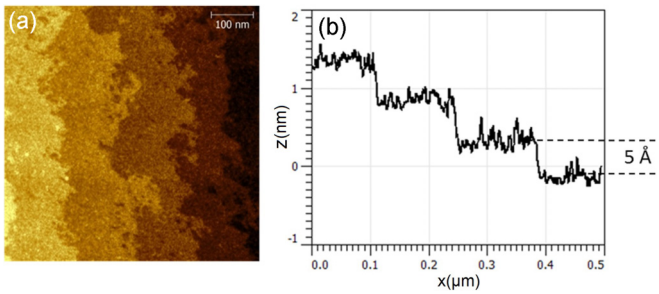

FIG. 1. (a) Ambient AFM image of the β-Ga_2O_3 ($\bar{2}01$) sample. (b) Cross section of the AFM image from (a).

self-trapped heavy holes produced by charge pumping from the STM tip.

Stable STM images of β-Ga_2O_3 samples, like those shown in Figs. 2 and 3, were only obtained at negative sample bias polarity corresponding to a regime of hole injection into the sample [see Fig. 4(a)]. To further understand the physics of hole self-trapping, we performed tunnel bias cycling experiments. When the sample voltage is switched to positive polarity [switching to electron injection regime; see Fig. 4(b)], tunneling signals can only be observed during typically ~30–60 seconds (see Supplemental Material [22]). After this delay time (τ_a), an abrupt switching of the surface electronic properties takes place accompanied by a complete disappearance of tunneling signals (manifested as tip crush into the surface). Switching back to negative sample bias polarity restores the tunneling signals almost instantly, within $\tau_r \sim 0.1$ second. These measurements were performed many times, and the electronic switching effects were reproducibly observed. We attribute the first delay time (τ_a) to annihilation of self-trapped holes around the STM tip due to their recombination with injected electrons. The second, significantly shorter time τ_r can be attributed to an almost instant recovery of the positively charged surface layer when the holes are again being pumped into the sample. From these measurements, we may conclude that hole self-trapping and electron-hole recombination cross sections are likely to be in the ratio $\sim\tau_a/\tau_r \gg 1$. For typical currents used in our STM experiments, charge tunneling occurs with an interval of $\sim 10^{-8}$ sec, and the number of charges injected during 0.1 sec may be sufficient to populate a $10 \times 10\,\mu m^2$ surface area. The positively charged surface layer is anticipated to attract n-type carriers from the bulk (double charged layer) that significantly improves the electrical conductivity of the near-surface sample region and explains why stable STM imaging can only be performed under such conditions. The bistability at positive sample bias (with typical switching time ~minute) strongly resembles a bistability previously reported for Ga-terminated n-doped Si(111) [23], the effect that was also attributed to the formation of a dynamic charged layer at the surface.

In Fig. 5(a), we show the STM image obtained after a cycle of tunneling bias reversal. As we explained earlier, a bias reversal cycle most likely results in a total annihilation of the charged surface layer followed by its complete recovery. Therefore, it seems natural to anticipate some changes in the spatial distribution of trapped holes. Indeed, in Fig. 5(a), we now observe the formation of one-dimensional chains of self-trapped holes. The stripe order of the holes is manifested in the preferred direction of chains and equidistant spacing between the holes inside a chain. In Fig. 5(a), the 1D chains are directed ~45° with respect to the horizontal axis. The stripe order and preferred chain direction/periodicity can also be observed on the 2D STM Fourier transform in Fig. 5(b). For comparison, in Fig. 5(c), we show a typical 2D STM Fourier transform obtained before bias cycling and not containing any signatures of spatial order. The comparison of Figs. 5(b) and 5(c) clearly indicates that the rearrangement of holes takes place after a cycle of annihilation/recovery of the charged surface layer. The inset of Fig. 6 demonstrates another example of the spatial ordering of holes after a cycle of annihilation/repopulation of the charged surface layer. The distance between the holes inside a chain is 2.5 nm and the STM signal amplitude is 2 Å.

The STM literature is lacking previous reports of direct observation of self-trapped charges in semiconductors. In principle, such trapped charges are anticipated to produce significant (~Å) out-of-plane corrugations on STM images, associated mainly with charge-induced local Coulomb potentials. For comparison, the STM corrugation amplitudes observed for CDW can be as large as 2 Å [24]. In Ref. [10], STM signal modulation induced by surface Mott-Hubbard

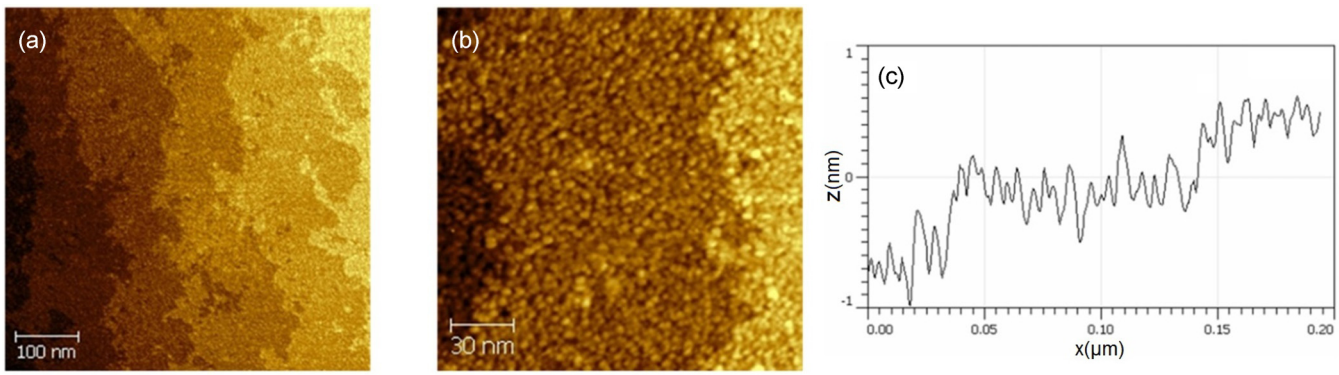

FIG. 2. (a),(b) Large-view STM images of the postannealed β-Ga_2O_3 ($\bar{2}01$) surface. The image size is (a) $560 \times 560\,nm^2$ and (b) $170 \times 170\,nm^2$. (c) STM cross section of (b) reveals 3-Å-height modulation with typical spatial periodicity of 3 nm developing on top of atomic terraces.

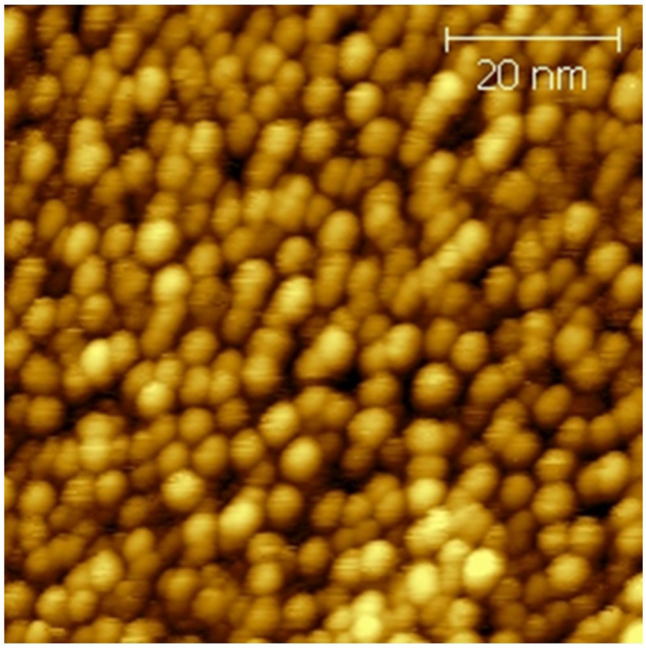

FIG. 3. STM image of the postannealed β-Ga_2O_3 ($\bar{2}01$) surface. The observed signal modulation does not reveal any visible spatial order. The image size is $74 \times 74\,\mathrm{nm}^2$. The image was obtained at 20 pA tunneling current and -4 V sample bias. The nearest-neighbor distance distribution here peaks around 3.5 nm, possibly indicating that some of the holes may be trapped below the surface and not visible on STM images.

CDW was less ($\sim$1 Å) due to efficient screening of Coulomb fields by subsurface charge carriers in the metallic sample. Therefore, the observed 2–3 Å signal amplitudes seem reasonable for β-Ga_2O_3. The saturated 2D hole density for the studied system can be estimated from the analysis of Coulomb interactions. In our model, the charge distribution in the sample includes the 2D surface layer of self-trapped holes and the complementary near-surface 2D layer of electrons attracted from the bulk. In view of electroneutrality, the 2D densities associated with holes and electrons are the same ($n_h = n_e = n$). As shown in the literature [25,26], screening of charged defects by 2D electron gas occurs on a length scale

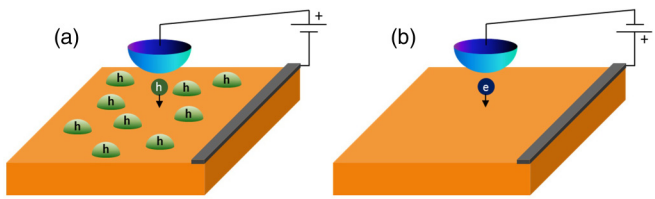

FIG. 4. (a) Formation of positively charged layer of self-trapped holes under negative sample bias polarity. Assuming significant hole trapping probability, for typical STM experimental conditions, such surface layer can be formed within $\sim$0.1 sec or even less. (b) For positive sample bias polarity, the 2D layer of self-trapped holes annihilates with injected electrons and completely disappears after macroscopic time $\sim$min. On both images, the gray stripe represents the surface contact to the sample.

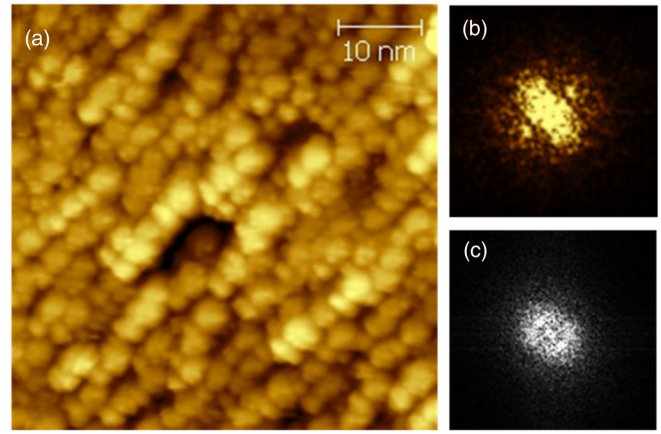

FIG. 5. (a) STM image of the β-Ga_2O_3 ($\bar{2}01$) surface obtained after a bias reversal cycle. The image size is $50 \times 50\,\mathrm{nm}^2$. The tunneling conditions are the same as for Fig. 3. The formation of one-dimensional chains is clearly observed. (b) Development of a stripe order after STM bias cycling was also confirmed by the 2D STM Fourier analysis. (c) 2D STM Fourier transform obtained *before* STM bias cycling.

of average distance between electrons, which for $n_h = n_e$ also represents the distance between the neighboring holes. Therefore, in a simplest model, Coulomb interaction between the nearest holes can be estimated as unscreened whereas interactions between higher-order neighbors should be set to zero. For an isolated hole, the self-trapping occurs due to competition of its self-trapping potential energy ($-U_0$) and its kinetic energy determined by the width of the valence band, which is known to be very narrow (<0.1 eV) for β-Ga_2O_3 [27]. Inside the charged surface layer, the effective trap depth decreases due to Coulomb repulsion between the holes. Since only nearest-neighbor interactions should be taken into account, the effective trap potential becomes

$$u(R) = -U_0 + N\,v(R), \tag{1}$$

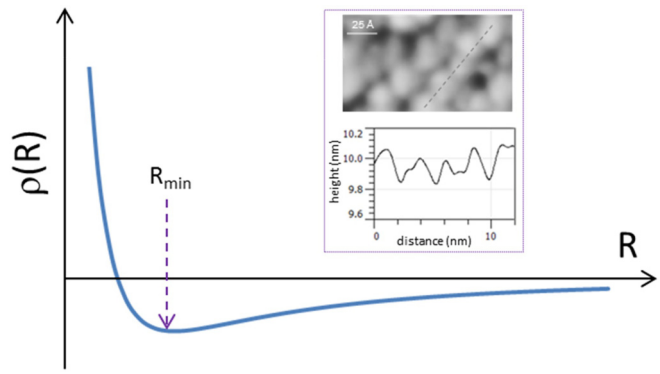

FIG. 6. The potential energy density $\rho(R)$ for an ensemble of interacting self-trapped holes plotted as a function of R. The potential energy minimum corresponds to $R = 3Nke^2/4\varepsilon U_0$. Inset: Another STM image and its cross section revealing the stripe order of holes. The spatial period inside a chain is $R = 2.5$ nm. The STM signal amplitude is 2 Å.

where $v(R) = ke^2/\varepsilon R$, k is Coulomb constant, N is a coordination number, and ε is a dielectric constant. For ε value exactly at the surface, we can use the average of its bulk ($\varepsilon_b \approx 10$) and vacuum values [19,28]. To obtain the total energy of the ensemble of interacting trapped holes, their Coulomb energies (v) should be summed over all neighboring pairs. Since the hole density is $\propto R^{-2}$, the total energy can be conveniently expressed through the 2D potential energy density:

$$\rho(R) \propto -\frac{U_0}{R^2} + \frac{1}{2}\frac{N\ v(R)}{R^2}. \quad (2)$$

The $\rho(R)$ dependence is presented in Fig. 6. The minimum of the total potential energy is anticipated to occur at

$$R_{\min} = 3Nke^2/4\varepsilon U_0. \quad (3)$$

For $R = 2.5$ nm determined from our STM data (see Fig. 6 inset), we find $U_0 \approx 0.5$ eV. Interestingly, the alternative estimation approach relying on $u(R) = 0$ yields $U_0 \approx 0.6$ eV. The thus obtained U_0 values are in good agreement with the previous modeling study, which predicted $U_0 \approx 0.53$ eV [11], indicating that our simple model properly captures the properties of an interacting ensemble of self-trapped holes [29]. Recently, the coexistence of Wigner crystallization and stripe order has been predicted for systems with nearly flat electronic bands [30], like a flat valence band in the studied material. According to the Ref. [30] analysis, the stripe order arises from the competition between hexagonal and square Wigner crystals due to spontaneous symmetry breaking caused by this competition. Besides the Coulomb interaction-induced mechanism, strong ordering tendencies for ensembles of interacting charged polarons were predicted at high densities due to long-range Peierls-like distortion [21]. The ordering densities in Ref. [21] are an order of magnitude higher than we observed. Thus, STM measurements on β-Ga_2O_3 reveal Wigner-Mott ordering of heavy holes induced by a classical Coulomb repulsion mechanism, whereas the higher 2D hole density regime predicted in Ref. [21] has not been observed.

In conclusion, the self-trapping of heavy holes in β-Ga_2O_3 has been confirmed using the STM technique. Both glassy and ordered striped phases of self-trapped holes have been observed, and the transition between these phases has been demonstrated. The possibility of erasing and repopulating the 2D layer of holes and thus inducing the spatial order is experimentally demonstrated here.

The authors thank Y. Bazaliy, K. Matveev, J. A. Gupta, A. Balatsky, J. Ferguson, A. Reed, M. McConney, and A. K. Roy for interesting discussions and help.

[1] E. Wigner, Phys. Rev. **46**, 1002 (1934).
[2] J. van den Brink, R. Eder, and G. A. Sawatzky, Europhys. Lett. **37**, 471 (1997).
[3] C. C. Grimes and G. Adams, Phys. Rev. Lett. **42**, 795 (1979).
[4] P. M. Platzman and M. I. Dykman, Science **284**, 1967 (1999).
[5] P. Glasson, V. Dotsenko, P. Fozooni, M. J. Lea, W. Bailey, G. Papageorgiou, S. E. Andresen, and A. Kristensen, Phys. Rev. Lett. **87**, 176802 (2001).
[6] H. Ikegami, H. Akimoto, and K. Kono, Phys. Rev. Lett. **102**, 046807 (2009).
[7] E. Rousseau, D. Ponarin, L. Hristakos, O. Avenel, E. Varoquaux, and Y. Mukharsky, Phys. Rev. B **79**, 045406 (2009).
[8] D. G. Rees, I. Kuroda, C. A. Marrache-Kikuchi, M. Höfer, P. Leiderer, and K. Kono, Phys. Rev. Lett. **106**, 026803 (2011).
[9] S. A. Lyon, Phys. Rev. A **74**, 052338 (2006).
[10] I. B. Altfeder and D. M. Chen, Phys. Rev. Lett. **101**, 136405 (2008).
[11] J. B. Varley, A. Janotti, C. Franchini, and C. G. Van de Walle, Phys. Rev. B **85**, 081109(R) (2012).
[12] N. Ma *et al.*, Appl. Phys. Lett. **109**, 212101 (2016).
[13] T. Oishi, Y. Koga, K. Harada, and M. Kasu, Appl. Phys. Express **8**, 031101 (2015).
[14] M. Higashiwaki *et al.*, Semicond. Sci. Technol. **31**, 034001 (2016).
[15] K. D. Chabak *et al.*, Appl. Phys. Lett. **109**, 213501 (2016).
[16] K. Sasaki, M. Higashiwaki, A. Kuramata, T. Masui, and S. Yamakoshi, J. Cryst. Growth **378**, 591 (2013).
[17] Y. Zhang *et al.*, Appl. Phys. Lett. **112**, 173502 (2018).
[18] Z. Galazka *et al.*, Cryst. Res. Technol. **45**, 1229 (2010).
[19] K. Irmscher, Z. Galazka, M. Pietsch, R. Uecker, and R. Fornari, J. Appl. Phys. **110**, 063720 (2011).
[20] C. T. Lee, H. W. Chen, and H. Y. Lee, Appl. Phys. Lett. **82**, 4304 (2003).
[21] C. Franchini, G. Kresse, and R. Podloucky, Phys. Rev. Lett. **102**, 256402 (2009).
[22] See Supplemental Material at http://link.aps.org/supplemental/10.1103/PhysRevB.98.241413 for bias cycling data are more STM images.
[23] I. B. Altfeder and D. M. Chen, Phys. Rev. Lett. **84**, 1284 (2000).
[24] I. Ekvall, H. E. Brauer, E. Wahlström, and Håkan Olin, Phys. Rev. B **59**, 7751 (1999).
[25] S. Das Sarma, Shaffique Adam, E. H. Hwang, and Enrico Rossi, Rev. Mod. Phys. **83**, 407 (2011).
[26] D. Jena, A. C. Gossard, and U. K. Mishra, Appl. Phys. Lett. **76**, 1707 (2000).
[27] H. He, M. A. Blanco, and R. Pandey, Appl. Phys. Lett. **88**, 261904 (2006).
[28] For a surface charge, half of the field lines go through the bulk and another half through vacuum. Therefore, the effective dielectric constant is the average of its bulk and vacuum values.
[29] The energy balance in Eq. (2) should also include the increase of 2D electron density for shorter hole-hole separation and the corresponding increase of kinetic energy. Estimations for β-Ga_2O_3 [11–20,27] show that the kinetic energy per electron is mainly determined by room temperature thermal energy (k_BT) and for estimation purposes this term can be omitted.
[30] B. Jaworowski, A. D. Güçlü, P. Kaczmarkiewicz, M. Kupczyński, P. Potasz, and A. Wójs, New J. Phys. **20**, 063023 (2018).